

PAPER • OPEN ACCESS

## Integration of the GET electronics for the CHIMERA and FARCOS devices

To cite this article: E De Filippo *et al* 2018 *J. Phys.: Conf. Ser.* **1014** 012003

View the [article online](#) for updates and enhancements.

### Related content

- [Flexible Electronics. Volume 1: The flexible electronics paradigm](#)  
V K Khanna
- [The Farcos project: Femtoscope Array for Correlations and Femtoscopy](#)  
G Verde, L Acosta, T Minniti et al.
- [Campaign of measurements to probe the good performance of the new array FARCOS for spectroscopy and correlations.](#)  
L. Acosta, R. Andolina, L. Auditore et al.



**IOP | ebooks™**

Bringing you innovative digital publishing with leading voices to create your essential collection of books in STEM research.

Start exploring the collection - download the first chapter of every title for free.

# Integration of the GET electronics for the CHIMERA and FARCOS devices

E De Filippo<sup>1</sup>, L Acosta<sup>1,8</sup>, L Auditore<sup>2,1</sup>, C Boiano<sup>3</sup>, G Cardella<sup>1</sup>,  
A Castoldi<sup>3,5</sup>, M D'Andrea<sup>1</sup>, S De Luca<sup>2,1</sup>, F Favella<sup>1</sup>, F Fichera<sup>1</sup>,  
N Giudice<sup>6,1</sup>, B Gnoffo<sup>6,1</sup>, A Grimaldi<sup>1</sup>, C Guazzoni<sup>3,5</sup>,  
G Lanzalone<sup>4,7</sup>, F Librizzi<sup>1</sup>, P Litrico<sup>4</sup>, C Maiolino<sup>4</sup>, S Maffesanti<sup>3,5</sup>,  
NS Martorana<sup>6,4</sup>, A Pagano<sup>1</sup>, EV Pagano<sup>4</sup>, M Papa<sup>1</sup>, T Parsani<sup>3,5</sup>,  
G Passaro<sup>4</sup>, S Pirrone<sup>1</sup>, G Politi<sup>6,1</sup>, F Previdi<sup>3,5</sup>, L Quattrocchi<sup>2,1</sup>,  
F Rizzo<sup>6,4</sup>, P Russotto<sup>4</sup>, G Saccà<sup>1</sup>, G Salemi<sup>6,1</sup>, D Sciliberto<sup>1</sup>,  
A Trifirò<sup>2,1</sup> and M Trimarchi<sup>2,1</sup>

<sup>1</sup> INFN, Sezione di Catania, Italy

<sup>2</sup> Dipartimento di Scienze MITF, Università di Messina, Italy

<sup>3</sup> INFN, Sezione di Milano, Italy

<sup>4</sup> INFN, Laboratori Nazionali del Sud, Catania, Italy

<sup>5</sup> Dip. di Elettronica, Informazione e Bioingegneria, Politecnico di Milano, Italy

<sup>6</sup> Dip. di Fisica e Astronomia, Università di Catania, Italy

<sup>7</sup> Università di Enna, "Kore", Italy

<sup>8</sup> Instituto de Física, Universidad Nacional Autónoma de México, México

E-mail: defilippo@ct.infn.it

**Abstract.** A new front-end based on digital GET electronics has been adopted for the readout of the CsI(Tl) detectors of the CHIMERA  $4\pi$  multi-detector and for the new modular Femtoscopy Array for Correlation and Spectroscopy (FARCOS). It is expected that the coupling of CHIMERA with the FARCOS array, featuring high angular and energy resolution, and the adoption of the new digital electronics will be well suited for improving specific future data analysis, with the full shape storage of the signals, in the field of heavy ion reactions with stable and exotic beams around the Fermi energies domain. Integration of the GET electronics with CHIMERA and FARCOS devices and with the local analog data acquisition will be briefly discussed. We present some results from previous experimental tests and from the first in-beam experiment (Hoyle-Gamma) with the coupled GET+CHIMERA data acquisition.

## 1. Introduction

The CHIMERA  $4\pi$  detector, originally conceived for multi-fragmentation and reaction dynamics studies in the Fermi energy domain [1, 2], has passed different upgrades, in agreement with new experimental and physical needs. The most recent one was the Silicon Pulse Shape upgrade (PSD) [3], aiming to measure the rise time of the signals for the charged particles stopping in the silicon detector (the first detection layer of the CHIMERA telescope). In this way the threshold for simultaneous mass and charge identification for light fragments was extremely lowered. This last aspect is particularly important when the isospin degree of freedom is investigated in nuclear reactions in order to study quantities related to the Equation Of State (EOS) of asymmetric nuclear matter and in-medium nuclear effective interactions [4, 5].



The availability of radioactive beams at LNS [6], that has also opened the use of CHIMERA detector to nuclear structure and clustering studies, requires new constraint in the particles detection, like the capabilities to detect with good efficiency, together with light charged particles,  $\gamma$ -rays and/or neutrons. Recently, the capability of the CHIMERA CsI(Tl) detectors for  $\gamma$ -rays identification was exploited in a study upon the 4.44 MeV excited level of  $^{12}\text{C}$  [7] and in the search of the isoscalar excitation of the Pygmy resonance in  $^{68}\text{Ni}$  [8].

Amongst other observables, two and multi-particle correlations are important tools to characterize the time scale and shape of emission sources in the dynamical evolution of heavy ion collisions. But this imposes both high energy and angular resolutions in particle detection. FARCOS is an ancillary and compact multi-detector with high angular granularity and energy resolution for the detection of light charged particles (LCP) and Intermediate Mass Fragments (IMF) designed for multi-particle correlation measurements and "femtoscopia" studies [9–11]. The FARCOS array is constituted by 20 telescopes in the final project. Each telescope is composed by three detection stages: the first  $\Delta E$  is a 300  $\mu\text{m}$  thick DSSSD silicon strip detector with 32x32 strips; the second is a DSSSD, 1500  $\mu\text{m}$  thick with 32x32 strips; the final stage is constituted by 4 CsI(Tl) scintillators, each one of 6 cm in length.

A single FARCOS telescope has to handle at least 196 readout channels taking into account a double amplification dynamics, limited to front strips. Thus the final FARCOS array needs to handle around 4000 channels. Moreover the electronic front-end of the 1192 CHIMERA CsI(Tl) scintillators, based on VME readout [12], was becoming obsolescent in the last ten years of successful runs. For these reasons a generic and scalable electronic system, covering digitalization, signals readout, synchronization and triggering based on the GET electronics (General Electronics for TPCs) [13, 14] has been adopted. The integration of this system has required the development of a new first stage front-end for FARCOS, based on CMOS new preamplifiers for both DSSSD Silicon [15] and CsI(Tl) detector [16], integrated in a single and compact ASIC board, and the design of a new dual-gain module to fit with the wide dynamical energy ranges expected for the CHIMERA CsI(Tl) and FARCOS Silicon detectors. Indeed a careful redesign of CHIMERA data acquisition was needed in order to couple the GET digital acquisition with Chimera Silicon detectors readout handled by the analog acquisition on VME bus.

In the following, only few selected aspects of the upgrade project will be shown, with particular emphasis on qualification of the GET electronics in particle identifications and data acquisitions integration.

## 2. Qualification of the GET electronics with CHIMERA detectors

The GET electronics, based on the integrated circuit AGET chip, originally designed for Time Projection Chambers (TPCs) and active targets devices has been adapted for CsI(Tl) scintillators and Silicon strip detectors of CHIMERA and FARCOS arrays. In particular the main idea was to by-pass the pre-amplification stage embedded in the AGET chip in order to use the existing CHIMERA pre-amplifiers operating under vacuum [17] and to design a new CMOS front-end in the Silicons and CsI(Tl) for the FARCOS array [15, 16]. Signals coming from the pre-amplifiers are interfaced to the GET system through a Dual Gain Module. This last is a multichannel digitally programmable gain amplifier, two ways splitter and level adapter, interfaced to the AGET inputs. In this way the large dynamic range of more than  $10^3$  required by CHIMERA and FARCOS devices can be achieved.

The GET electronics is described in detail in Ref. [14] and references therein. Very briefly, the AGET chip integrates 64 channels with a pre-amplifier, an analog filter (shaper) and leading-edge discriminator. Four further channels, Fixed-Pattern Noise (FPN), are used to evaluate the intrinsic noise level and baseline shape of the channels. The filtered signals are sampled trough storing in a analog memory based on a Switched Capacitor Array (SCA) structure (512-cell

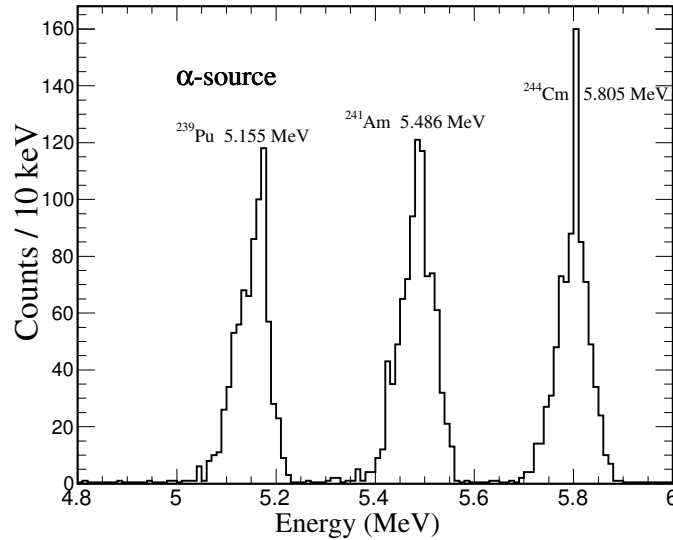


**Figure 1.** Energy spectrum of a three peaks  $\alpha$  source relative to a single strip (front side) of a 1500  $\mu\text{m}$  thick DSSSD strip detector of a FARCOS telescope, obtained by 50 MS/s digitized pulses.

deep) and codified by a 12 bit ADC. A sampling rate up to 100 MS/s can be set-up. Four AGET chips are arranged in a card called AsAd (ASIC and ADC) that acts as a front-end for the GET system. Up to 4 AsAd board (1024 channel) can be connected to the CoBo board that manages the slow control of the AGET chips and the readout of the AsAd(s) data at a maximum bandwidth of 1.2 Gb/s for each AsAd. CoBo boards are housed in a  $\mu\text{TCA}$  (Micro Telecom Computing Architecture) crate together with the trigger box, “MuTanT”. A  $\mu\text{TCA}$  crate can handle up to 11 CoBo boards and it handles also the data sending to a computer farm for data analysis and storage through the Ethernet link backplane at 10 Gb/s maximum bandwidth.

In order to characterize the GET electronics for CHIMERA and FARCOS devices an extensive testing phase has been performed during the hardware and software upgrade developments. We show in this section some selected results of this preliminary phase. Fig. 1 shows the energy spectrum of a mixed nuclei (three peaks)  $\alpha$  source irradiating under vacuum a DSSSD strip detector, 1500  $\mu\text{m}$  thick, 64x64 mm<sup>2</sup> dimension, of a FARCOS telescope. The spectrum is relative to one strip of the detector front side. In this test the detector was coupled to a commercial (Mesytec) charge pre-amplifier ( $\sim 13$  mV/MeV) followed by a Dual Gain module (gain = 2) interfaced to the AsAd input. The digitized output is filtered with the AGET front-end analog filter with a peaking time of 1  $\mu\text{s}$  and digitized at 50 MS/s in the SCA to be codified by a 12 bit ADC. The output waveforms are software analyzed (FPN subtraction, baseline restore, digital filtering with a Finite impulse Response (FIR) triangular filter, see Refs. [18–21] for an overview of typical digital signal processing with CHIMERA detectors) in order to perform on-line and off-line computation on the pulse waveform. Fig. 1 presents the spectrum distribution of the signal pulse height and shows a resolution of 60-70 keV (FWHM) that is on average when operating on this kind of detectors by using GET electronics at 50 MS/s and commercial pre-amplifiers.

We have performed different tests under Tandem and Cyclotron beams at LNS in order to check the GET electronic in standalone mode (not coupled with CHIMERA data acquisition)

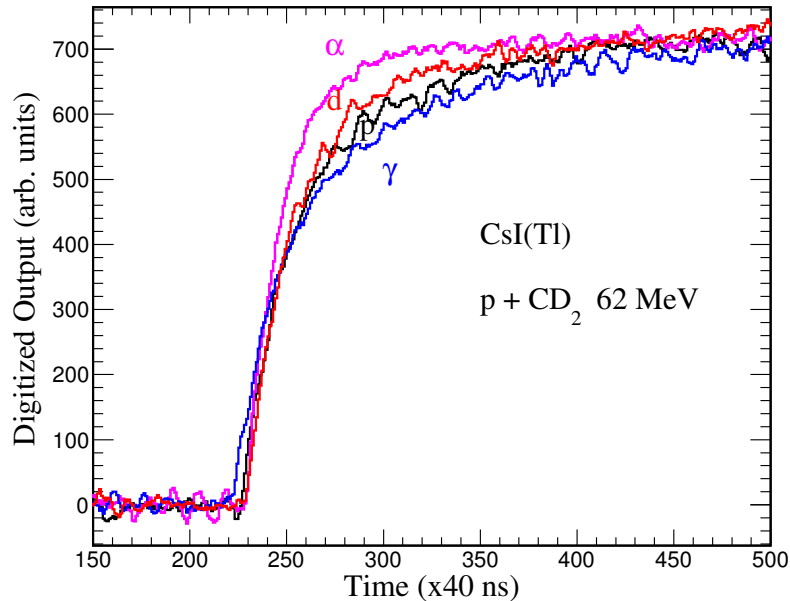


**Figure 2.** Baseline subtracted output waveforms (unfiltered), collected at 25 MS/s, for different light charged particles and  $\gamma$ -rays detected by a CHIMERA CsI(Tl) of ring 9 (R9-37E,  $\theta=28.5^\circ$ ) in the reaction  $p+CD_2$  (deuterated polyethylene target) at 62 MeV (see text for details).

with the CHIMERA telescopes, for both Si and CsI(Tl) detectors. In one of the performed tests we used a proton (62 MeV) beam and some telescopes of ring 9 ( $\theta=28.5^\circ$ ) by using the standard CHIMERA pre-amplifiers for Silicons and CsI(Tl) detectors, these last with photodiode readout of the light output. Signals from Si and CsI(Tl) were both digitized at the relative low frequency of 25 MS/s (40 ns step) in this experiment, mostly devoted to CsI(Tl) response. The CsI(Tl) signal was shaped with the AGET Sallen-Key filter with a small peaking time (220ns), so preserving the rise time information. CsI(Tl) light particles and  $\gamma$  identification was obtained by calculating the pulse height (PH) vs. the Rise Time of the signals read at the output of the pre-amplifiers. This identification technique has been shown to be equivalent to the conventional Fast-Slow components scatter plot of the light emission [18]. Fig. 2 shows a sample of signals of different particles (p,d, $\alpha$ ,  $\gamma$ -rays), identified in the PH vs Rise-Time scatter plot and having approximately the same pulse heights. The waveform outputs shown in the figure were baseline restored; no software FIR filter was applied. This collection of traces nicely shows how faster is the light collection for  $\alpha$  particles in CsI(Tl) with respect to deuterons, protons and  $\gamma$ -rays respectively, giving the possibility of an off-line optimization of the identification procedures.

We have performed tests under beam with CHIMERA detectors and GET in standalone trigger mode during the CLIR (Clustering in Light Ions Reactions) experiment [22,23] with the FRIBs (in Flight Radioactive Ions BeamS) facility at LNS. A fragmentation cocktail beam was produced starting from a 55 MeV/nucleon  $^{18}O$  primary beam impinging on a 1.5 mm thick  $^9Be$  target for fragments production. The cocktail beams, collected after the fragments separator, are sent to the reaction target inside the vacuum chamber. The CHIMERA tagging system can select, event-by-event, each incoming isotope [24]. Ions like  $^{10,11}Be$ ,  $^{13}B$  and  $^{16}C$  were produced with an average  $10^4$ - $10^5$  pps rate depending on selected ion.

In this experiment some telescopes of the ring 2 of CHIMERA ( $\theta = 4^\circ$ ) were connected

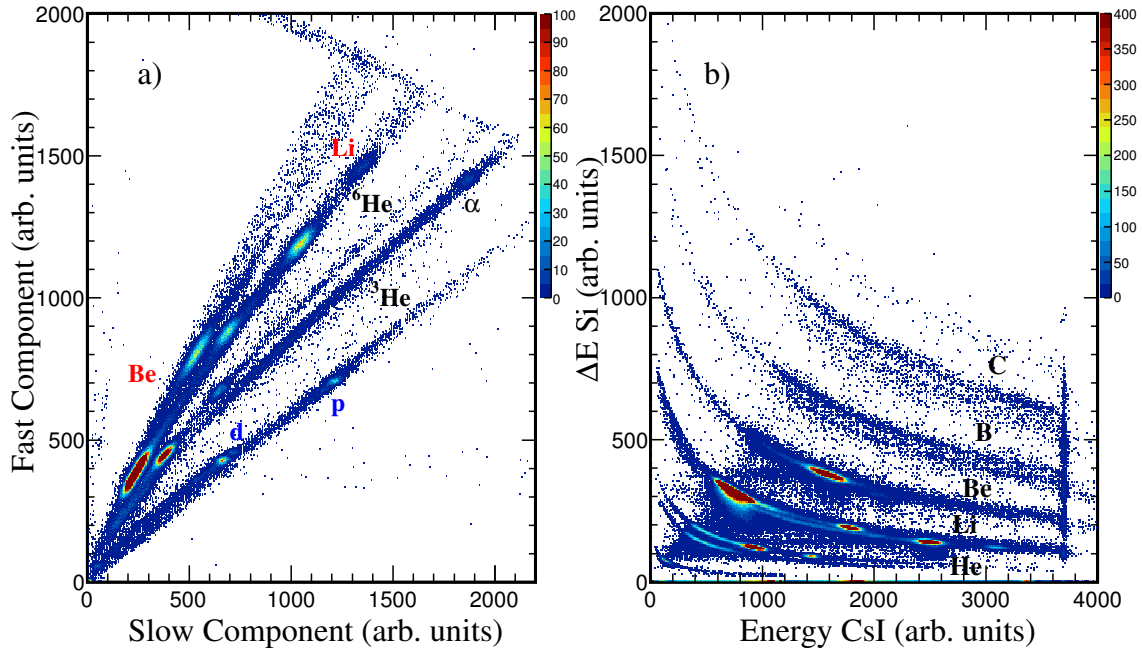


**Figure 3.** Data obtained with GET electronics and data acquisition for reaction products on a telescope of ring 2 (R2-18E,  $\theta=4^\circ$ ) from a cocktail beam on a thin polyethylene  $(\text{CH}_2)_n$  target. a) Fast vs. Slow component identification in CsI(Tl) detector. b) Particle identification from the  $\Delta E$  energy loss in the 300  $\mu\text{m}$  Silicon detector vs the residual energy in CsI(Tl) detector. In these plot bumps are of course relative to the elastic peaks of the cocktail beams

to the GET electronics with the purpose to compare results with those from standard analog acquisition. Fig. 3 show results of particles identification obtained with the GET system. A 50  $\mu\text{m}$  thick polyethylene  $(\text{CH}_2)_n$  target was used in the shown data. We tested in different runs a sampling rate of 25 or 50 MS/s for both Silicon and CsI(Tl) detectors (when using a single CoBo a unique sampling rate can be selected for all channels). Fig. 3 refers to the 25 MS/s sampling rate setting. CsI(Tl) fast and slow components, CsI(Tl) and Si pulse heights and rise times were calculated on the digitized outputs. For the determination of the Fast and Slow components, shown in Fig. 3a), we used the gates definition method described in Fig. 1 of Ref. [18], best suited for signals coming directly from a pre-amplifier output. In this method the Fast (Slow component) is obtained as the pulse value interval ( $H_2 - H_1$ ) corresponding to a given time window gate, ( $t_2 - t_1$ ). The time gate are 800 ns and between 1.4  $\mu\text{s}$  and 10  $\mu\text{s}$  respectively for the Fast and Slow component in Fig. 3a), calculated respect to the starting point (10% of the pulse height) of the signal. Fig. 3b) shows the Silicon Pulse Height distribution (Si energy loss) as function of the Csi(Tl) pulse height distribution (residual energy). It is interesting to note that, despite the poor sampling rate for a silicon detector, a good resolution is obtained for isotopic separation up to Carbon. This result for detectors of ring 2 in Chimera, that have just a 2 mV/MeV gain silicon pre-amplifier, is generally not reached with standard analog acquisition also in this range of low charge ions. Indeed a saturation in the CsI(Tl) light output is clearly seen in both bidimensional plots. Thus we argue that recovering the full energy range dynamic requires the use of the Dual Gain module.

### 3. Integrations of the data acquisitions

A part of the CHIMERA  $4\pi$  detector, limited to CsI(Tl) detectors, will use the GET front-end electronics as well the FARCOS telescopes. On the other hand the current electronic and readout front-end for Silicon detectors are expected to continue to be used. The actual electronic chain for CHIMERA Silicon detectors has, as final element, the analog codifiers (QDC and TDC, respectively Charge and Time to Digital convertes) housed in the VME bus. The total number of GET channels for the CHIMERA + FARCOS (20 telescopes) devices is around 6000. This number corresponds to about 24 AsAd distributed up to 8 CoBo modules. Thus, a single  $\mu$ TCA crate can handle the whole configuration. The GET data acquisition (based on CoBo readout modules and the MuTanT trigger in the  $\mu$ TCA bus) is described in detail in Refs. [13, 14].

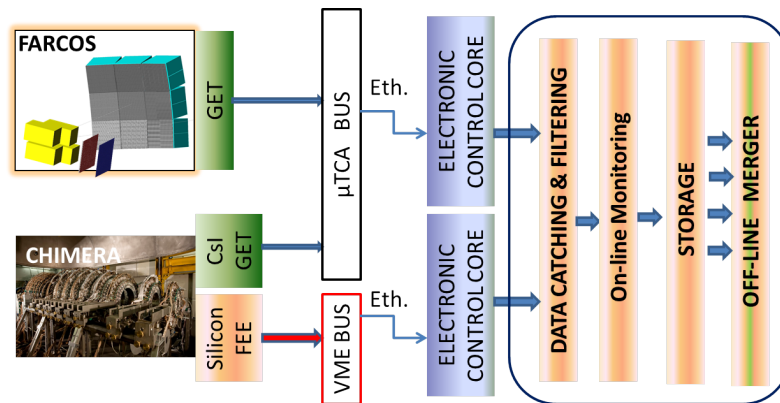


**Figure 4.** Schematic view of CHIMERA CsI(Tl) (GET), CHIMERA Silicon (VME DAQ) and FARCOS DAQ (GET) coupling. See text for details.

Fig. 4 shows schematically the data flow from the front-end electronics to the data storage. Initial tasks are the data collection from the readout server (for the VME bus) and the CoBo boards (for GET). Intermediate tasks are data filtering and on-line monitoring. Data storage and merging of the data belonging to the same event (event building) are the final tasks. We use, in order to manage all these tasks (excluding the data merging) the distributed acquisition framework NARVAL [25]. A NARVAL process, called “actor” is a task serving a specific function in the data flow. Both CHIMERA data acquisition and the GET one are supervised and coordinated by the NARVAL system.

The DAQ coupling is related on the use of a common trigger configuration. In this case the data merger among different acquisitions can be easily based on Timestamps and/or event number that has to be the same for a each event generated by the same trigger in different acquisition systems. The MuTanT trigger handles a Global Master Clock (GMC) at 100 MHz synchronizing all CoBo modules belonging to same crate and the 14 bit Timestamp recorded in each single CoBo. The MuTanT has three trigger levels (L0, L1, L2). L0 is an external trigger (for example generated by CHIMERA silicon detectors in our case); L1 is generated by the internal total multiplicity, derived by the sum of the individual channel multiplicities in all AsAd devices; L2 is a user software implemented trigger. Unfortunately there is no compatible Timestamp device on the CHIMERA VME bus. Therefore the merging between the VME events and the GET ones is handled by using the event counter that essentially acts as a trigger number counter both in VME and GET systems. Note that the method of common trigger and event counter can be successfully used only if the DAQ dead time is shared between the two different data acquisitions, handling in a proper way the busy signal from the different DAQ and front-end systems.

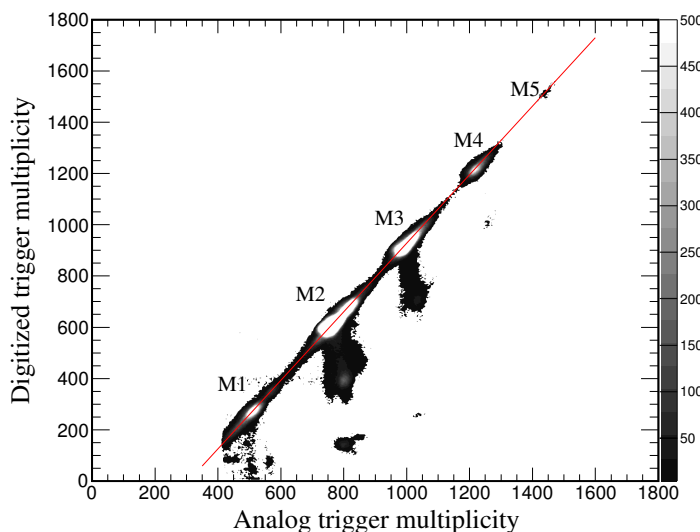


**Figure 5.** 2D plot showing the correlation between the analog sum multiplicity signal distribution generated by the CHIMERA Silicon detectors and sent: in Y-axis to a channel of the GET system, to be analyzed by the digital DAQ; in X-axis to a QDC channel in the VME bus to be integrated by the analog DAQ. Correlated events with the same event number should stay along a diagonal line.

In the event builder the fact that two events coming from the VME and GET buffer respectively have the same event counter is only a necessary condition but not sufficient in order to affirm that the two events are correlated. In order to monitor, event-by-event, the data correlation we use the procedure described in Fig. 5. The multiplicity signal (analog sum signal) generated by the CHIMERA constant fraction discriminators for Silicon detectors is integrated in a QDC channel of the VME DAQ. The same signal is splitted, sent to an AsAd channel of the GET electronics and analyzed in pulse height for each valid trigger. The correlation between the two distributions after the event building have to lay in a diagonal line (as shown in Fig. 5). Conversely it will show a random behaviour for runs with uncorrelated events.

In order to perform the event building a new application called "DataMerger" has been developed [26]. The DataMerger manages data collected by CoBo(s) in the GET digital acquisition and VME analog DAQ and merges data belonging to the same trigger/event on the basis of the timestamp and/or event number. The DataMerger is also an on-line or off-line program for data analysis and signal processing. In fact, the DataMerger does not work directly upon raw data frames in order to do merging, but at the level of pre-analysed data collected for each single partial event. In this way the final results of the merging action are physical raw data that are ready to be stored in Root trees [27] or spectra for on-line and off-line monitoring. Fig. 6 shows the logical data flow of the application. The program generally collects data stored on disk on several files created by each Narval Storage Actor that are related to each CoBo present in the data acquisition and to VME data flow, because no merging is performed at DAQ level. Of course each stored file contains only data related to the single CoBo (or VME). Note that in this way the data storage is faster because it is distributed on different tasks and files equal to the number of different CoBo modules (plus the VME Daq buffers) used.



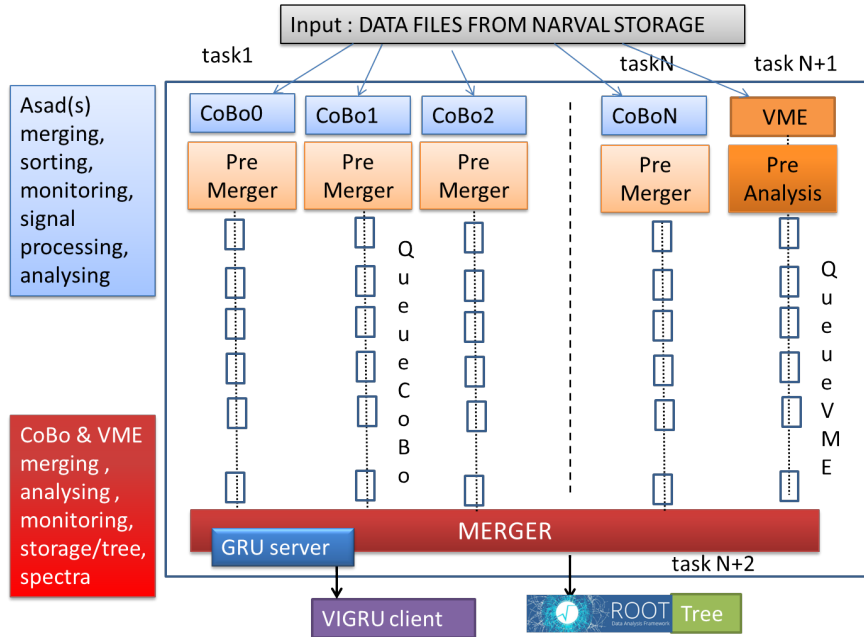


**Figure 6.** Data flow of the Merger application for CHIMERA-GET event building. Computation of digitized waveforms and AsAd frames merging (pre-merger) belonging to a given CoBo are done by single tasks concurrency running on separate threads. ViGRU [28] is a client for on-line visualization of Root histograms.

#### 4. The Hoyle-Gamma experiment

The GET integration in CHIMERA detectors has been validated in November 2017 during the Hoyle-Gamma experiment at LNS. The goal of this experiment was to search for the  $\gamma$ -decay branching ratio of the 7.65 MeV Hoyle state and the rare  $\gamma$ -decay modes in  $^{12}\text{C}$ , in particular, the  $3_1^-$  state at  $E_x = 9.64$  MeV [29–31], whose  $\gamma$ -decay probability is very small and poorly known.

In the experiment a  $^4\text{He}$  (64 MeV) ions beam delivered by the Superconducting Cyclotron at INFN-LNS was used, impinging on a thin  $^{12}\text{C}$  target. The main idea of this experiment was to exploit the  $4\pi$  coverage of the CHIMERA detector to detect and identify, by using the CsI(Tl) scintillators, the  $\gamma$ -ray cascade relative to the decay of the 7.65 Hoyle and the 9.64 excited levels in  $^{12}\text{C}$  and to detect in coincidence the inelastic scattered  $\alpha$  particles and the  $^{12}\text{C}$  recoil nucleus [7, 32]. The kinematical coincidence technique should permit also to extract meaningful angular distributions for  $\gamma$ -rays as shown in Ref. [7].

In the experiment the GET digital electronics was used for the readout of the all CsI(Tl) scintillators of the CHIMERA backward part (the Sphere,  $30^\circ < \theta < 176^\circ$ ). Dual Gain modules were used to split all CsI signals in two different gains in particular in order to improve the signal to noise ratio for the low energies  $\gamma$ -rays. Signals coming from the Sphere pre-amplifiers were splitted by 8 Dual Gain modules (around 1000 channels) and sent to 4 AsAd distributed over 2 CoBo modules for data readout. A remaining 2 AsAd connected to a third CoBo were used for control and monitoring purposes. All signals were sampled at 50 MS/s. The remaining CsI(Tl) of the CHIMERA forward part and the Silicon detectors were readout with the usual electronic front-end and analog readout in the VME bus. Events were triggered requiring a multiplicity  $M \geq 2$  in the Silicon detectors. The multiplicity signal was sent to the L0 input (external trigger) of the MuTanT trigger box. The acquisition rate was around 1 kHz and all the sampled signals

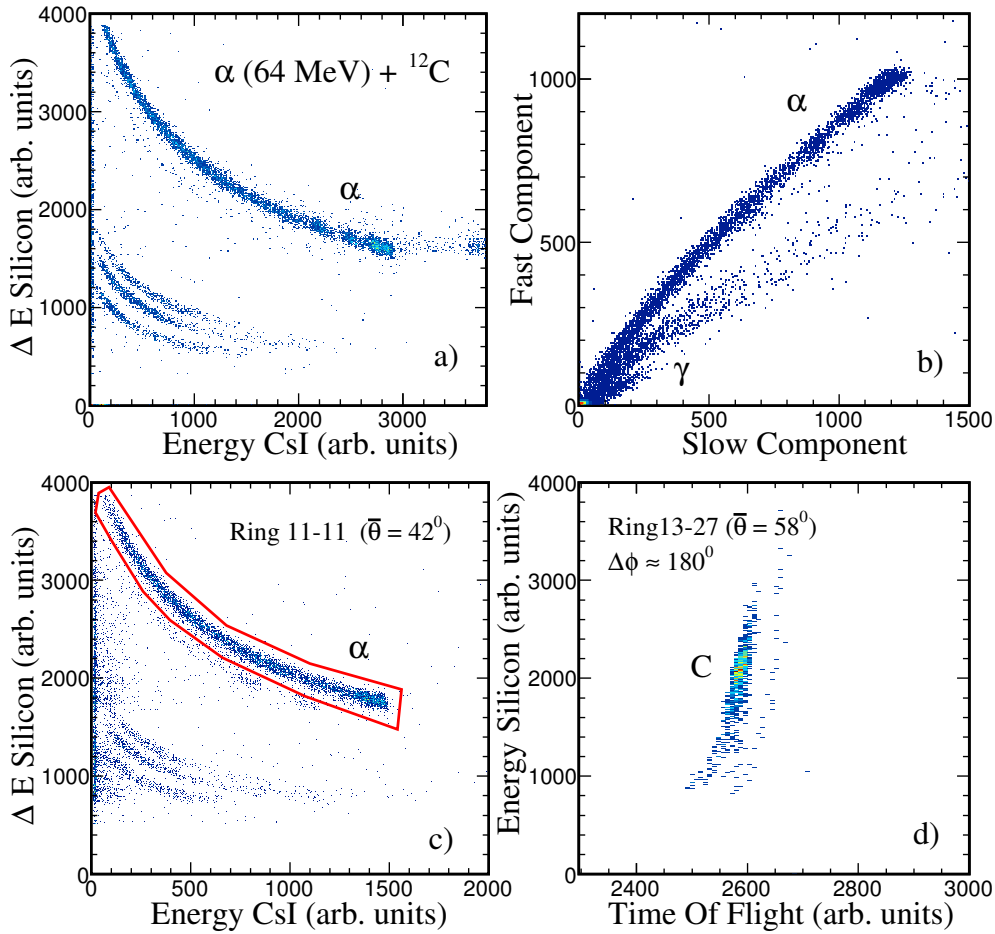


**Figure 7.** a)  $\Delta E$ -E bidimensional plot for a telescope of ring 10 in the CHIMERA sphere; b) the corresponding Fast-Slow component of light emission in the CsI(Tl) 2D plot; c)  $\Delta E$ -E bidimensional plot for a telescope of ring 11. d) Energy vs Time-of-Flight 2D plot obtained imposing a kinematical coincidence between the  $\alpha$  selected by a cut in Fig. 7c) and a telescope of ring 13 with a  $\Delta\phi \approx 180^\circ$ , showing the Carbon recoil.

from CsI(Tl) detectors were stored on disk. A maximum total rate of 150 MB/s of stored data was reached during the acquisition.

The data analysis requires as first step an accurate calibration of CsI(Tl) and Silicon detectors that is not yet available. We show a sample of first results in Fig. 7. Fig. 7a) shows the  $\Delta E$  energy loss in Silicon vs. residual energy in CsI for a CHIMERA telescope of ring 10 ( $\theta = 34^\circ$ ). In this bidimensional plot the  $\Delta E$  is obtained by the analog front-end and VME DAQ while the x-axis (residual energy) is obtained by the pulse height distribution of the relative CsI(Tl) channel in the GET digital electronic. Fig. 7b) shows the corresponding Fast vs. the Slow component bidimensional plot giving  $\gamma$  and light particles identification in CsI(Tl) obtained by pulse shape analysis of the sampled data. Finally we tested the coincidences of (in)-elastically scattered  $\alpha$  particles with  $^{12}\text{C}$  recoils that is one of the task of the experiment. Selecting alpha particles in a telescope of ring 11 (Fig. 7c)) we expect the maximum yield for the  $^{12}\text{C}$  recoil in a telescope of ring 13 with an azimuthal angle difference between the two telescopes of  $\Delta\phi \approx 180^\circ$ .

The Carbon recoil stops in the Silicon detector, thus can be only detected by Time-of-Flight technique. This is well shown in Fig. 7d) where the Silicon energy vs. the Time-of-Flight (determined respect the Cyclotron Radio-Frequency) is plotted.

The examples shown in Fig. 7 give a first view of the general correctness of the adopted procedures in the upgrade phase and during the experiment and they are a good start for the prosecution of the data analysis.

## 5. Conclusion

Following the building of a first FARCOS module demonstrator and the approval for the construction of 5 FARCOS modules (20 telescopes) we have adopted a compact electronic front end based on the design of new ASIC preamplifiers for silicon strips and FARCOS CsI(Tl) and the GET electronics for digitalization and data readout. The front-end for CsI(Tl) CHIMERA detectors has been upgraded by using GET electronic as well.

A CHIMERA-GET hybrid data acquisition and the new Dual Gain modules designed at INFN-Catania have been successfully tested during the Hoyle-Gamma experiment.

The main goal for the next future is that the FARCOS ancillary detector, with its high energy and angular resolution, can enhance the physics that can be studied with the CHIMERA array (including two and multi-particles correlations) both with stable and radioactive beams, in the field of dynamics of heavy ion collisions and spectroscopy of light nuclei in the vicinity of drip lines. In view of this goal, studies to include also the neutron detection in CHIMERA and FARCOS have been recently started [33] in order to provide unique information about nuclear dynamics and spectroscopy working with exotic and stable beams.

## References

- [1] Pagano A 2012 *Nuclear Physics News* **22**,1 25
- [2] De Filippo E and Pagano A 2014 *Eur. Phys. J. A* **50** 32
- [3] Alderighi M et al. 2005 *IEEE Trans. Nucl. Sci.* **52** 1624
- [4] Horowitz C et al. 2014 *J. Phys. G* **41** 093001
- [5] Oertel M, Hempel M, Klahn T and Typel S 2017 *Rev. Mod. Phys.* **89** 015007
- [6] Russotto P et al. 2018 Contribution to this conference
- [7] Cardella G et al. 2015 *Nucl. Instrum. Meth. Phys. Res. A* **799** 64
- [8] Martorana N S et al. 2018 *submitted to Phys. Lett. B*
- [9] FARCOS Technical Design Report 2015, available on-line at:  
<https://drive.google.com/file/d/0B5CgGwz8Lp00c3pGTWd0cDBoWFE>
- [10] Pagano E V et al. 2016 *EPJ Web of Conf.* **117** 10008
- [11] Acosta L et al. 2016 *J. Phys.: Conf. Series* **730** 012001
- [12] Alderighi M et al. 2002 *Nucl. Instrum. Meth. Phys. Res. A* **489** 257
- [13] Giovanazzo J et al. 2016 *Nucl. Instrum. Meth. Phys. Res. A* **840** 15
- [14] Pollacco E C et al. 2018 *Nucl. Instr. Meth. Phys. Res. A* **887** 81
- [15] Castoldi A, Guazzoni C and Parsani T 2014 *Proc. IEEE Nucl. Sci. Symp. Med. Imag. Conference, Seattle Wa, Nov. 2014* 1-5
- [16] Castoldi A, Guazzoni C and Parsani T 2017 *IEEE Trans. Nucl. Sci.* **64** 2678
- [17] Bassini R, Boiano C, Pagano A, Pullia A 2004 *IEEE Trans. Nucl. Sci.* **51** 115
- [18] Acosta L et al. 2013 *IEEE Trans. Nucl. Sci.* **60** 284
- [19] Amorini F et al. 2007 *IEEE Trans. Nucl. Sci.* **54** 208
- [20] Amorini F et al. 2012 *IEEE Trans. Nucl. Sci.* **59** 1772
- [21] De Luca S 2016 Doctoral Thesis, Catania University
- [22] Dell'Aquila D et al. 2016 *Phys. Rev. C* **93** 024611
- [23] Dell'Aquila D et al. 2017 *Acta Phys. Polonica B* **48** 499
- [24] Lombardo I et al. 2011 *Nucl. Phys. (Proc. Suppl.) B* **215** 272
- [25] X. Grave et al 2005 *Proc. 14th IEEE Real Time Conference* 119
- [26] De Filippo E 2017 DataMerger: an object oriented Merger for CHIMERA-GET data acquisition: User's Guide.
- [27] Brun R and Rademakers F 1997 *Nucl. Inst. and Meth. in Phys. Res. A* **389** 81
- [28] Legeard L *GRU/ViGRU documentation: <http://wiki.ganil.fr/gap/wiki/Documentation/Software/Gru>*

- [29] Tsumura M et al. 2014 *Jour. of Phys.: Conf. Series* **569** 012051
- [30] Alsharani B et al. 2013 *EPJ Web of Conferences* **63** 01022
- [31] Cardella G et al. 2017 *EPJ Web of Conferences* **165** 01009
- [32] Cardella G et al. 2016 Measurement of the  $\gamma$ -decay branching ratio of the Hoyle and first excited  $3^-$  levels of  $^{12}\text{C}$ . *Experiment proposal PAC-LNS/2016*
- [33] Pagano E V et al. 2018 *Nucl. Instrum. Meth. Phys. Res. A* **889** 83